COMPARISON OF FEA FIELD MODELS COMBINED WITH ANALYTICAL METHOD TO DETERMINE THE PERFORMANCE CHARACTERISTICS OF HIGH EFFICIENCY INDUCTION MOTORS

Victor P. B. Aguiar, Ricardo S. T. Pontes, Tobias R. Fernandes Neto and Kleymilson N. Souza
Federal University of Ceará, Electrical Engineering Department, Fortaleza – Ceará, Brazil
e-mail: victorpba@dee.ufc.br,ricthe@dee.ufc.br, tobias@dee.ufc.br, kleymilson@dee.ufc.br

***Abstract* –This paper proposes a comparison among FEA field models combined with analytical model, in order to predict with better accuracy the NEMA/IEC performance indicators. Such indicators are the locked-rotor current, efficiency, breakdown torque and locked-rotor torque. The Stationary (S), Time-Harmonic (TH) and Time-Stepping (TS) models have been compared with different simulation features, such as: linear (L) or nonlinear (NL) magnetic material, and with or without an external circuit coupled (C) to the FEA field model (effects of stator circuit). Benchmarks have been calculated by using nameplate and manufacturer data and compared with impedance tests and the method F1 from IEEE 112/2004 to measure efficiency and the breakdown torque. Regarding both no-load and locked-rotor analyses, seven simulation tests were carried out. As result, the S model (no-load) and the NL-TH-C (locked-rotor) have the best accuracy in predicting the performance indicators NEMA/IEC.**

***Keywords* –finite element analysis, harmonic analysis, no-load test, locked-rotor test, torque calculation, transient analysis.**

NOMENCLATURE

X_m/ L_{m0}	Magnetizing reactance/inductance.
λ_m	Magnetizing linkage flux.
R_c	Core resistance.
$L_{l,2D}$	2D leakage inductance.
$R_{r,2D}$	2D rotor resistance.
W_m	Magnetizing energy.
P_r	Rotor losses.
$\vec{H}$	Magnetic field intensity.
$\vec{B}$	Magnetic density flux.
$\vec{A}$	Magnetic vector potential.
$\vec{J}$	Current density.
v	Magnetic reluctivity.
A_z	Magnetic vector potential stationary – z axis.
J_z	Current density stationary – z axis.
v_e	Magnetic effective reluctivity.
$\tilde{A}_z$	Magnetic vector potential phasor – z axis.
$\tilde{J}_z$	*Current density phasor – z axis.*
s	*Slip.*
ω	*Electrical frequency.*
σ	*Conductivity.*
t	*Time.*
Δt	*Time step.*
$L_{ls,3D}$	*Stator 3D leakage inductance.*

I. INTRODUCTION

Minimum efficiency performance standards (MEPS) for industrial electric motors are presented to the world community through standards as in [1] to U.S.A, in [2] to the European Union and in [3] to Brazil. In the last years, the MEPS have been under constant review. The motor efficiency classes to electric motors designed for operation on sinusoidal voltage and single speed are defined as IE1, IE2, IE3 e IE4 [2] or High efficiency, Premium Efficiency and Super Premium Efficiency [1]. The Brazilian standard [3] provides only the classes IE2 or 'High Efficiency' ('IR2' in Brazil) and IE3 or Premium Efficiency ('IR3' in Brazil). All standards aforementioned do not present new performance characteristics, such as: minimum/maximum breakdown torque, locked-rotor current and torque and the motor temperature rise, for the new concepts of efficiency classes. Moreover, manufacturing techniques which improve the efficiency, impose limits to pursue higher efficiency levels [4]-[6]. Some ideas related to the improvements in efficiency through stator losses reduction have been presented in [7]-[8], however, without experimental testing [7]-[8]. Furthermore, they did not discuss the impact of the efficiency improvements in the performance characteristics.

High-efficiency motors available in the market have been designed based on careful modifications in all productive chains, so that the increased efficiency does not increase the cost in the final product [6] [9] [10]. High-efficiency NEMA motors or similar are designed with closed rotor slots. Rotor slots totally closed have well-known features such as: better rotor die-cast aluminum injection [11], reduced noise, reduced iron losses [12] [13] and a slighter increase in the leakage flux due to slot rotor bridge, reducing the current harmonics for inverter fed motors [13]. Such kind of slot has shown a non-linear behavior in the voltage-current curve during the locked rotor test [14], turning it hard to model in the equivalent motor circuit.

Finite element analysis (FEA) in induction motors (IM) is a step towards the modern design of induction motors [15] and it has been used for different purposes [16] [17]. FEA can be carried out in two ways [18]: 1) acquiring the equivalent circuit parameters through simulations of the no-load and locket rotor tests and then applying those simulated parameters to calculate indirectly the torque, as shown in Figure 1 [16] [19], 2) adding in the finite element motor model the 3D motor effects like: the end winding inductance, and then its determine the torque directly [17] [20].

Recent researches are focusing on these specific parameters of the induction motor equivalent circuit, such as: leakage slot inductance and leakage differential inductance,

978-1-4799-8779-5/15/$31.00 ©2015 IEEE

by means of new FEA techniques [21] [22]. Nevertheless, there is no comparison between the FEA Field Models (e.g. Time-Harmonic or Time-Stepping), in order to simulate the indirect and direct tests about the influence of the performance characteristics in high efficiency motors. The features of each kind of FEA field models change the simulated parameters during the indirect tests.

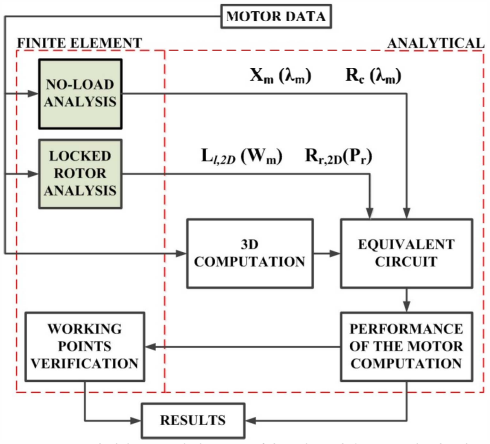

Fig. 1. FEA Field Model Combined with Analytical Method Scheme [16].

Therefore, the main purpose in this paper is to compare the Time-Harmonic (TH) and Time-Stepping (TS) FEA field models using a non-linear Magnetic Material (B-H Curve) [17]. FEA field models will be simulated with and without an external circuit coupled to the stator (C) [18]. All results from the FEA field models, which simulate the no-load and locked-rotor tests, will be analyzed by an analytical method to calculate the motor's performance characteristics [16]. The models used to simulate the no-load and the locked-rotor tests will be compared by a simple approach error. Nameplate and manufacturer data like stator resistance, stator sheet, rotor sheet, wire diameters, number of turns/phase, type of magnetic material, winding type and rotor ring dimensions are used to modeling the FEA field models and the analytical method. Initial benchmarks are calculated from the aforementioned data, but experimental measurements should be taken as a benchmark as well.

II. ANALYTICAL AND FEA FIELD MODELS COMBINATION

The section presents briefly the concepts of the FEA field models.

A. Finite Element Method (FEM)

The finite element method is a numerical technique for finding approximate solutions to boundary value problems for partial differential equations (PDE), which uses the variational or residual methods [19] [20] [23] [24]. The most commonly used residual method is the Garlekin [23]-[24]. In summary, the 2D FEM steps are based on:

1) Mesh model: It consists of generating a mesh with a finite number of triangular elements or quadrilateral elements in the problem domain, hence it is important the constructive details of the designed motor, such as the slot shape [24]. To simulate a 2D induction motor (IM), only the cross-section of the machine is considered.

2) Maxwell's Equations: The equations which describe the magnetic phenomena at low frequencies are given as follows:

$$\nabla \times \vec{\boldsymbol{H}} = \vec{\boldsymbol{J}} \tag{1}$$

$$\vec{\boldsymbol{H}} = \nu \vec{\boldsymbol{B}} \tag{2}$$

$$\vec{\boldsymbol{B}} = \nabla \times \vec{\boldsymbol{A}} \tag{3}$$

From (1), (2) e (3) the eq. (4) is determined.

$$\nabla \times \left(\nu \cdot \nabla \times \vec{\boldsymbol{A}} \right) = \vec{\boldsymbol{J}} \tag{4}$$

The vertex of each element are related with $\boldsymbol{A}$, from the (x,y) position through shape functions [23]. The shape functions will not be presented, since it is out of scope of this work. The magnetic vector potential of the element is given by the weighted sum of each vertex potential values:

$$A(x,y) = \sum_{i=1}^{k} \phi_i(x,y) A_i \tag{5}$$

where:

$A(x,y)$ – Element magnetic vector potential;
A_i – Vertex potential at i;
ϕ_i – Vertex shape function at i;
k – Number of vertex of the element.

3) Reluctivity Matrix: The reluctivity matrix should be quadratic and sparse [23] [24] and there is an overlap in the magnetic effects over a single element. Equation (6) is utilized to solve FEM problems.

$$[S]_{nxn} \cdot [A_n]_{n\times 1} = [J]_{n\times 1} \tag{6}$$

where:

$[S]$ – Reluctivity matrix;
$[A_n]$ – Vector of potentials of each element;
$[J]$ – Sources input vector of each element;
n – Number of elements.

B. Stationary Field Modeling (S)

Stationary field model is the simplest FEA field model. In fact, the S-model only calculates the magnetic flux densities at several points of the model, confirming the initial designed densities.

Considering, the source (current density $\boldsymbol{J}$) constant and located in the z axis [20] [23]-[24], and the field in the xy plane, eq.(4) can be rewritten as (7) for this field model.

$$\frac{\partial}{\partial x}\left(\nu \frac{\partial A_z}{\partial x} \right) + \frac{\partial}{\partial y}\left(\nu \frac{\partial A_z}{\partial y} \right) = -J_z \tag{7}$$

For each model element, we should set the reluctivity (ν) and current density (*J*) to solve it. Furthermore, it can be used a linear or nonlinear magnetic material.

B. Time Harmonic Field Modeling (TH)

In time harmonic field modeling, the sources are sinusoidal waveforms [19] [20] [23]-[24] and the magnetic vector potential is time-varying [23]-[24]. The current density in (1), is the sum of the external and the induced current densities. Considering the phasor quantities and substituting it in (4), we obtain eq. (8).

$$\frac{\partial}{\partial x}\left(\nu_e \frac{\partial \tilde{A}_z}{\partial x}\right)+\frac{\partial}{\partial y}\left(\nu_e \frac{\partial \tilde{A}_z}{\partial y}\right)-j(s\sigma)\omega\tilde{A}_z=-\tilde{J}_z \quad (8)$$

The term related to the induced current is shown and it is function of the electrical frequency, conductivity and slip, turning the model a predictor of the induced currents in the rotor bars. The model does not estimate the magnetic saturation of the material, and then the effective reluctivity is used. The stored energy method is used to establish the B-H curve of the material in the nonlinear case [17] [20]-[21].

C. Time-Stepping Field Modeling (TS)

Since, time-varying sources produces time-varying magnetic fields [19] [20] [23]-[24]. The main equation of this modeling is presented in (9).

$$\frac{\partial}{\partial x}\left(\nu \frac{\partial A_z}{\partial x}\right)+\frac{\partial}{\partial y}\left(\nu \frac{\partial A_z}{\partial y}\right)-s\sigma\frac{\partial A_z}{\partial t}=-J_z(t) \quad (9)$$

The discrete time equation of (9) is given in (10). Therefore, it is obtained the time-stepping model equation.

$$\frac{\partial}{\partial x}\left(\nu\frac{\partial A_Z(t+\Delta t)}{\partial x}\right)+\frac{\partial}{\partial y}\left(\nu\frac{\partial A_Z(t+\Delta t)}{\partial y}\right)-s\sigma\frac{A_Z(t+\Delta t)}{\Delta t}=\cdots \quad (10)$$

$$\ldots=-s\sigma\frac{A_Z(t)}{\Delta t}-J_Z(t+\Delta t)$$

As result, the reluctivity matrix is assembled for each time interval with an additional term related to the actual simulated induced currents. However, there is an additional term related to previous simulated induced currents in the sources vector.

D. External Circuit Coupled in the Field Model (C)

The external coupling circuit turns the numerical model more flexible to indirect tests (no-load and locked-rotor). In fact, the external circuit turns the circuit current another variable [23]. Considering the turns density per area as a function of the current and the current density, eq. (9) can be rewritten in (11).

$$\frac{\partial}{\partial x}\left(\nu \frac{\partial A_z}{\partial x}\right)+\frac{\partial}{\partial y}\left(\nu \frac{\partial A_z}{\partial y}\right)-s\sigma\frac{\partial A_z}{\partial t}+w_1 I=0 \quad (11)$$

where:

w_1 – Turns density per area;
I – Current.

The coupled stator circuit equation is given in (12).

$$W_1\frac{\partial A_z}{\partial t}l+L_{ls,3D}\frac{dI}{dt}+R_s I=U(t) \quad (12)$$

where:

W_1 – Turns per phase;
l – Axial core length.
R_s – stator winding resistance.
U – Input voltage.

Equations (11) and (12) should be formulated from the chosen model (TH or TS) and solved simultaneously [23].

E. Analytical Method and NEMA/IEC Performance Indicators

The analytical method (AM) for the IM performance calculation is obtained from the motor impedances [25]. The breakdown torque, locked-rotor current and locked-rotor torque are functions of the variables presented in (13), (14) and (15) respectively.

$$T_{bk} \propto \frac{1}{R_s+\sqrt{R_s^2+\left(\sum X_l\right)^2}} \quad (13)$$

where:

T_{bk} – Breakdown torque;
X_l – Total leakage reactance.

$$I_{lr} \propto \sqrt{\frac{1}{\left(R_s+R_r^S\right)^2+\left(\sum X_l^S\right)^2}} \quad (14)$$

where:

I_{lr} – Locked-rotor current;
X_l^S – Total leakage reactance in starting.
R_r^S – Rotor resistance in starting.

$$T_{lr} \propto \left(R_r^S I_{lr}^2\right) \quad (15)$$

where:

T_{lr} – Locked-rotor torque.

The efficiency (η) is calculated segregating completely the losses in the calculation procedure described in [25]. Then, it is possible to verify the importance of the leakage reactances and rotor resistance predictions either in nominal or starting condition.

III. SIMULATION TEST PROCEDURES

The simulated tests are the no-load and the locked-rotor (60 and 15 Hz) tests. The locked-rotor with a supply frequency of 15 Hz is used, in order to fulfill the method n°1 of the impedance tests described in [26]. The supply frequency of 60Hz determines the impedances during the starting. The simulations described in this section were performed by COMSOL *Multiphysics*.

A. Test Simulations nº I

In these simulations the test is performed only for no-load condition to obtain the flux density in air gap, the flux density in the teeth and yoke. All impedances are calculated by AM and we can consider this set nº I as an improved AM.

B. Test Simulations nº II, III, IV and V

The tests simulation II, III, IV and V are based on the no-load test by S model and the locked-rotor test with time-harmonic modeling [16] [19]. The difference between the simulations II, III, IV and V is the use of a linear magnetic material (II and IV), the use of a nonlinear magnetic material (III and V) and the stator external circuit coupled to the model (IV and V).

In the simulation of the no-load test, the S modeling is maintained because the flux density in the air gap was neglected (unfeasible flux density value due to spatial harmonics). Therefore, it is used the magnetizing inductance determined in the no-load test to extract parameters from the circuits depicted in Figure 2.

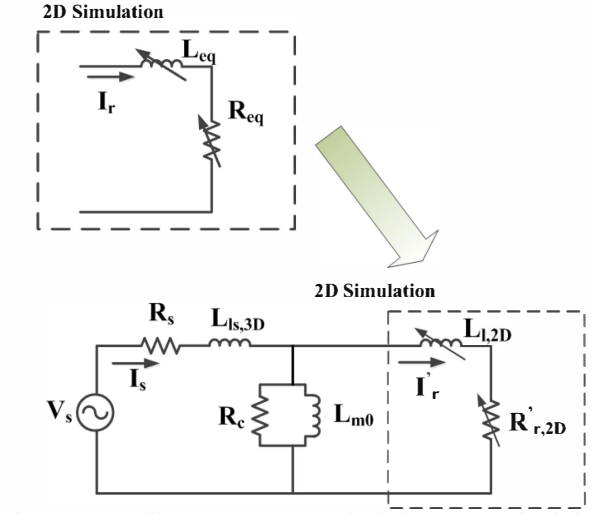

Fig. 2. Extracting parameters from locked-rotor 2D Simulation - Influence of magnetizing reactance [16] [19].

An extra simulation was carried out in IV and V; it is applied the method described in [21] for the 2D leakage reactance of the stator. It simulates the no-load test using TH modeling considering no slip.

C. Test Simulations nº VI and VII

Both locked-rotor test and no-load, for the tests simulation VI e VII, uses the time-stepping modeling and it was considered only nonlinear material. For these simulations, the process to extract the locked-rotor parameters can be achieved by using the magnetizing reactance, obtained in the locked-rotor test simulation.

The Test VII uses the stator external circuit to the model. Despite of that an extra simulation (no-load test and TH model) is carried out to determine the 2D stator leakage reactance, as shown previously. The results of the TS model are not satisfactory without modeling the rotor bars, since it reduces the total motor impedance. Moreover, it increases the magnetizing current in the simulation. Table 1 summarizes the simulated tests for the described models.

TABLE I
Summary of proposed simulation tests

Test Sim. nº	I	II	III	IV	V	VI	VII
No-Load	S	S	S	S/TH-C	S/TH-C	NL-TS	NL-TS/TH-C
Locked Rotor	-	L-TH	NL-TH	L-TH-C	NL-TH-C	NL-TS	NL-TS-C

IV. TEST RESULTS

The motor under test has 1.5 HP, 2 poles, 380 V and 2.32 A of rated current. It is connected in star connection and it is classified as “High Efficiency” or “IE2” (‘IR2’ in Brazil). Figure 3 shows the cross-sectional view of the motor.

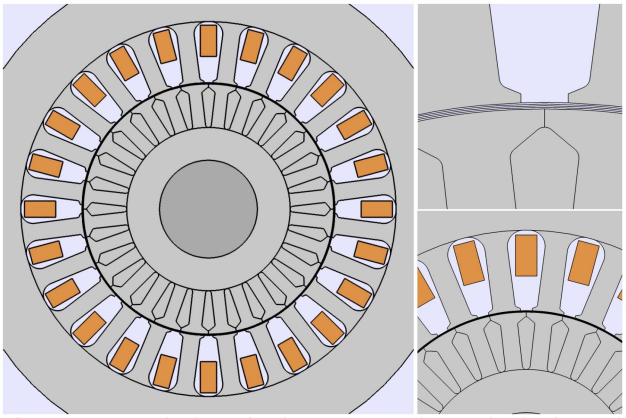

Fig. 3. Motor under investigation – Rotor and stator lamination and constructive details (right).

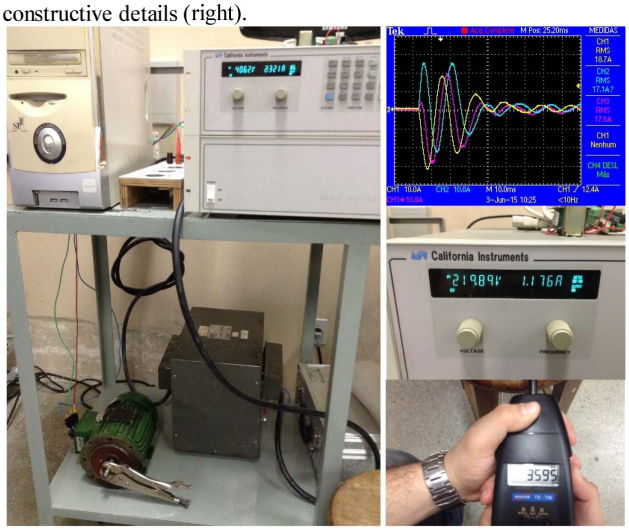

Fig. 4. Testing workbench during locked-rotor test (left), no-load test (lower right) and starting currents (upper right).

The experimental tests are carried out in order to calculate the equivalent circuit parameters to the efficiency method F1 [26]. For the impedance tests used to calculate the circuit

TABLE II
Benchmark values: nameplate (NP), IEEE/112-Method F1 (F1) and locked-rotor current measurement

Induction Motor: 1,5 HP – 2 poles, 380 V / 60 Hz, 3400 RPM							
η (%)		T_{BK} (N.m)		I_{LR} (A)		T_{LR} (N.m)	
Benchmark NP	**83.0**	Benchmark NP	**9.3**	Benchmark NP	**17.4**	Benchmark NP	**9.6**
Benchmark F1	**83.0**	Benchmark F1	**8.8**	Benchmark M	**17.8**		
Error	-	Error	**-5.4 %**	Error	**2.3 %**	Error	-
IE2 eff. Class> 82.5%		*NEMA/IEC design > 5.6 N.m*		*NEMA/IEC design < 25.1 A*		*NEMA/IEC design > 5.0 N.m*	
Min. Abs. Error: -0.5%		*Min. Error (%): -39.7%*		*Max. Error (%): 44.2%*		*Min. Error (%): -47.9%*	

parameters (method 1, 2, 3 and 4), only the method 4 does not necessitate the supply frequency be up to 15 Hz. Table II compares the benchmarks calculated through the nameplate and manufacturer's data (NP) and the benchmarks calculated by the method F1 [26]. Method F1 does not calculate starting performance characteristics. Figure 4 shows the testing workbench to proceed with all test and measurement.

V. SIMULATION RESULTS

From the results shown in Table III, it can be concluded that the stationary (S) for the no-load analysis and the nonlinear time-harmonic with external stator circuit couple model (NL-TH-C) for the locked-rotor analysis have the best accuracy to predict the equivalent circuit parameters with lower error for the locked-rotor torque and current among the field modeling combined with analytical method.

Stator circuit coupled in TH model predicts lower error for 2D leakage reactance of stator therefore predicts starting indicators NEMA/IEC successfully according to (14) and (15). Estimating error of reactance is slightly greater than 20% however the error of starting indicators NEMA/IEC is slightly greater than 10%. There is an improvement in the values estimated by TH-C compared to L-TH or NL-TH.

However, they have high errors for the efficiency and the breakdown torque. The predicted rotor resistance error is equal to 14% for the TH-C model, which suggests a weak estimation to the rotor losses because the error is equal to 28% (therefore it prejudices the estimation of motor efficiency). Estimated breakdown torque has an error of 38.6% and prediction error in leakage reactance sum is 36.3%.

In TS models, the estimation error of rotor losses is around 70% as well as the error in rotor resistance prediction. About the weak estimation of the 2D rotor resistance in the TS modeling highlights that the circuit parameter extracts only the fundamental air-gap flux density, where there is a strong influence of the harmonics during the calculation of the 2D rotor resistance.

Error in sum of leakage reactance is around 50% as well as the breakdown torque prediction error (nº VII). Starting indicators NEMA/IEC have the biggest errors than simulations nº VI and lead us to predict that simulation nº VII has biggest errors on sum of starting leakage reactances and starting resistance rotor.

VI. FINAL REMARKS

The test simulation nº V has shown the best accuracy compared to all tests. The comparison between the experimental measured benchmarks shows that the test simulation nº V maintains the best accuracy to the most of performance characteristic (NEMA/IEC design). Table II confirms again the best accuracy of the test simulation nº V for the calculated values from nameplate and manufacturer data, except breakdown torque (test simulation nº IV).

For all no-load test simulations the rotor speed was neglected. According to [27], the speed produces several harmonics in the air-gap flux density, increasing the core losses. As future work, we intend to simulate the no-load test VII using the TS modeling, with linear material, without external stator circuit and the rotor at synchronous [27].

The coupling of the external stator circuit predicts efficiently the 2D leakage reactance of the stator, as

TABLE III
Comparing AM/FEA with benchmark values calculated by tests

Induction Motor: 1,5 HP – 2 poles, 380 V / 60 Hz, 3400 RPM													
	Efficiency			**Breakdown Torque**			**Locked rotor Current**			**Locked rotor Torque**			
η (%)	A.M.	84.6	T_{BK} (N.m)	A.M.	12.6	I_{LR} (A)	A.M.	19.2	T_{LR} (N.m)	A.M.	10.0
	Abs. Error	1.6		Error (%)	43.2		Error (%)	7.4		Error (%)	4.2
	I	84.6		I	13.5		I	20.3		I	11.2
	Abs. Error	1.6		Error (%)	53.4		Error (%)	14.0		Error (%)	16.7
	II	86.9		II	17.8		II	30.1		II	7.2
	Abs. Error	3.9		Error (%)	102.3		Error (%)	69.1		Error (%)	-25.0
	III	86.9		III	17.8		III	30.1		III	7.3
	Abs. Error	3.9		Error (%)	102.3		Error (%)	69.1		Error (%)	-24.0
	IV	84.4		IV	**12.2**		IV	20.6		IV	11.7
	Abs. Error	1.4		Error (%)	**38.6**		Error (%)	15.7		Error (%)	21.9
	V	**84.0**		V	12.3		V	**20.5**		V	**11.6**
	Abs. Error	**1.0**		Error (%)	39.8		Error (%)	**15.2**		Error (%)	**20.8**
	VI	85.9		VI	15.6		VI	24.7		VI	8.1
	Abs. Error	3.0		Error (%)	77.3		Error (%)	38.8		Error (%)	-15.6
	VII	85.9		VII	13.8		VII	24.8		VIII	7.0
	Abs. Error	3.0		Error (%)	56.8		Error (%)	39.3		Error (%)	-27.1
Benchmark		**83.0**	Benchmark		**8.8**	Benchmark		**17.8**	Benchmark		**9.6**
IE2 eff. Class > 82.5%			*NEMA/IEC design > 5.6 N.m*			*NEMA/IEC design < 25.1 A*			*NEMA/IEC design > 5.0 N.m*		
Min. Abs. Error: -0.5%			***Min. Error (%): -37.8%***			***Max. Error (%): 41.0%***			***Min. Error (%): -47.9%***		

Bold marked values depict the models with the smallest error compared with the benchmark value and Underline marked values depict the models with unacceptable error (compared with minimum error or maximum one)

described in [21]. This feature is important to design or repair the winding of an IM [7] [8].

The simulation of no-load test by TS modeling with external stator circuit and rotor circuit included in the numerical model will be next step, since the lack of rotor circuit in motor 2D model decreases total impedance and the no-load current becomes larger than expected. Other next step towards the tests simulation nº VII is to check the influence of the harmonics in rotor resistance and the 2D leakage reactance.

ACKNOWLEDGEMENTS

The authors thank CENAPAD/UFC for computational support. This project is financially supported by the CNPq (process: 459091/2014-0).

REFERENCES

[1] *ANSI Motors and Generators*, NEMA Std. MG-1, 2014.

[2] *IS Rotating Electrical Machines: Efficiency classes of line operated AC motors (IE code)*, IEC Std. 60034-Part 30-1, 2014.

[3] *NBR Rotating Electrical Machines – Induction Motors: Polyphase*, ABNT Std. 17094-Part 1, 2013.

[4] A. Boglietti, A. M. El-Refaie, O. Drubel, A. M. Omekanda, N. Bianchi, E. B. Agamloh, M. Popescu, A. Di Gerlando, and J. B. Bartolo, "Electrical Machine Topologies – Hottest Topics in the Electrical Machine Research Community", *IEEE Industrial Electronics Magazine*, vol. 8, nº 2, pp. 18-30, Jun. 2014.

[5] L. Albertini, N. Bianchi, A. Boglietti, A. Cavagnino, "Core Axial Lengthening as Effective Solution to Improve the Induction Motor Efficiency Classes", *IEEE Transactions on Industry Applications*, vol. 50, nº 1, pp. 218-225, Jan/Feb.2014.

[6] A. Boglietti, A. Cavagnino, L. Ferraris, M. Lazzari, G. Luparia, "No Tooling Cost Process for Induction Motor Energy Efficiency Improvements", *IEEE Transactions on Industry Applications*, vol. 41, nº 3, pp. 808-816, May/Jun.2005.

[7] V. P. B. Aguiar, R. S. T. Pontes, T. R. Fernandes Neto, "Study and Energy Efficiency Improvement in the Design of an Induction Motor based on Interactive CAD Software", *in Proc. of COBEP*, vol. 01, pp. 878-883, 2013.

[8] L. Zhang, Y. Huang, J Dong, B. Guo, T. Zhou, "Stator Winding Design of Induction Motors for High Efficiency", *in Proc. of ICEMS*, vol. 01, pp. 130-134, 2014.

[9] A. Boglietti, A. Cavagnino, L. Ferraris, G. Luparia, "Induction motor efficiency improvements with low additional production costs", *in Proc. of PEMD*, vol. 02, pp. 775-780, 2004.

[10] I. Torac, "A few aspects concerning the squirrel cage induction motors efficiency improvement", *in Proc. of OPTIM*, vol. 01, pp. 740-744, 2012.

[11] T. S. Birch, O. I. Butler, "Permeance of closed-slot bridges and its effect on induction-motor-current computation", *Proceedings of the IEE*, vol. 118, nº 1, pp. 169-172, Jan. 1971.

[12] K. Delaere, R. Belmans and K. Hameyer, "Influence of Rotor Slot Wedges on Stator Currents and Stator Vibration Spectrum of Induction Machines: A Transient Finite-Element Analysis", *IEEE Transactions on Magnetics*, vol. 39, nº 3, pp. 1492-1494, May 2003.

[13] W. Tong, *Mechanical Design of Electric Motors*, CRC Press, 1ª Edição, Boca Raton, 2014.

[14] A. Boglietti, A. Cavagnino, M. Lazzari, "Modelling of the closed rotor slot effects in the induction motor equivalent circuit", *in Proc. of ICEM*, vol. 01, pp. 1-4, 2008.

[15] E.B. Agamloh, A. Cavagnino, "High efficiency design of induction machines for industrial applications", *in Proc. of WEMDCD* vol. 01, pp. 33-46, 2013.

[16] L. Albertini, N. Bianchi, S. Bolognani, "A Very Rapid Prediction of IM Performance Combining Analytical and Finite-Element Analysis", *IEEE Transactions on Industry Applications*, vol. 44, nº 5, pp. 1505-1512, Sep./Oct.2008.

[17] T. Schuhmann, B. Cebulski, S. Paul, "Comparison of time-harmonic and transient finite element calculation of a squirrel cage induction machine for electric vehicles", *in Proc. of ICEM* vol. 01, pp. 1037-1043, 2014.

[18] K. Hameyer, J. Driesen, H. De Gersem, and R. Belmans, "The Classification of Coupled Field Problems", *IEEE Transactions on Magnetics*, vol. 35, nº 3, pp. 1618-1621, May 1999.

[19] N. Bianchi, *Electrical Machine Analysis using Finite Elements*, CRC Press, 1ª Edição, Boca Raton, 2005.

[20] K. Hameyer and R. Belmans, *Numerical Modelling and Design of Electrical Machines and Devices*, WIT Press, 1ª Edição, Southampton, 1999.

[21] Z. Ling, L. Zhou, S. Guo, Y. Zhang, "Equivalent Circuit Parameters Calculation of Induction Motor by Finite Element Analysis", *IEEE Transactions on Magnetics*, vol. 50, nº 2, #7020604, Feb.2014.

[22] O. Chiver, L. Neamt, C. Barz and D. Pop, "Torque-Slip Characteristic of Squirrel Cage Induction Motor by New FEA Technique", *in Proc. of COMPUMAG* vol. 01, pp. 779-780, 2013.

[23] J. P. A. Bastos and N. Sadowski, *Electromagnetic Modelling by Finite Element Methods*, Marcel Dekker, 1ª Edição, New York, 2003.

[24] M. N. O. Sadiku, *Numerical Techniques in Electromagnetics with MATLAB*, CRC Press, 3ª Edição, Boca Raton, 2009.

[25] I. Boldea and S. A. Nasar, *The Induction Machines Design Handbook*, CRC Press, 2ª Edição, Boca Raton, 2010.

[26] *IEEE Test Procedure for Polyphase Induction Motors and Generators*, IEEE Std. 112-1996, 2004.

[27] K. Komeza, M. Dems, "Finite-Element and Analytical Calculations of No-Load Core Losses in Energy-Saving Induction Motors", *IEEE Transactions on Industry Electronics*, vol. 50, nº 7, pp. 2934-2946, Jul. 2012.